

Flashpoint

D. Lynden-Bell^{1*} and H.K.Moffatt^{2†}

¹ *Institute of Astronomy, Madingley Road, Cambridge CB3 0HA, United Kingdom*

² *DAMTP, Centre for Mathematical Studies, Wilberforce Road, Cambridge, CB3 0WA*

Received 2015 April 20

ABSTRACT

A small electrically conducting sphere contains a dynamo source of magnetic field which externally has quadrupolar symmetry. It is surrounded by a force-free medium of finite electrical conductivity. Differential rotation of the sphere, together with a ‘solar wind’ blowing off it, can maintain a twisted force-free external field despite the ohmic dissipation; differential rotation alone cannot do so. Increasing differential rotation can lead to a rotating almost radial field that extends to ever greater distances, coupled with a strongly dissipative conical current sheet separating regions of outgoing and incoming field. Dissipation in the sheet prevents the field from reaching the critical twist angle (flashpoint) at which all the flux would extend to infinity. A thin current sheet of this kind is susceptible to resistive instabilities; possible consequences are discussed in the concluding section.

Key words: MHD: magnetic fields: magnetic reconnection: plasmas: galaxies – jets.

1 INTRODUCTION

A one-parameter family of self-similar axially symmetric force-free magnetic fields was derived by Lynden-Bell & Boily (1994) (hereafter L-B&B) who showed that a quadrupole field can withstand a twist of only $2\pi/\sqrt{3}$ ($= 208^\circ$) before a ‘flashpoint’ occurs, at which it develops a conical current sheet extending radially to infinity; beyond this critical twist, the meridional part of the field is purely radial. The cone has semi-angle $\pi/3$, dividing the upper hemisphere into regions of equal solid angle of outgoing and incoming field. The meridional ingredient of the field near to the critical condition is shown in Fig. 1; there is also a corresponding azimuthal field component concentrated near the current sheet.

L-B&B (see also Aly 1995) also noted that a *dipole* field outside a sphere can withstand a twist of only π before forming an equatorial current sheet extending to infinity, again dividing the available sky

into equal solid angles containing outgoing and incoming fields. Gourgouliatos (2008) derived a corresponding family of solutions within a cone of semi-angle θ_c , which again develop current sheets around an interior cone bounding half the solid angle available. Again the magnetic field extends radially to infinity once a critical twist is passed. The critical angle of twist is $\pi/\sqrt{1 - (1 + \cos\theta_c)^2/4}$, consistent with the above situations when $\theta_c = \pi/2$ and $\theta_c = \pi$. These field structures were described as being relevant to solar arcades and coronal mass ejections from the Sun.

Such fields extending to infinity provide examples of phenomena anticipated earlier through the energy theorems of Aly (1984), and in subsequent work (Aly 1994) where he used the method of L-B&B to find exact solutions to two-dimensional sheared arcades. In contrast to the axisymmetric situation, these arcades exhibit no critical behaviour, although increasing continuously in height with increasing shear. The difference can be understood by contrasting the energies of fields along the coor-

* E-mail:dlb@ast.cam.ac.uk

† E-mail:hkm2@damtp.cam.ac.uk

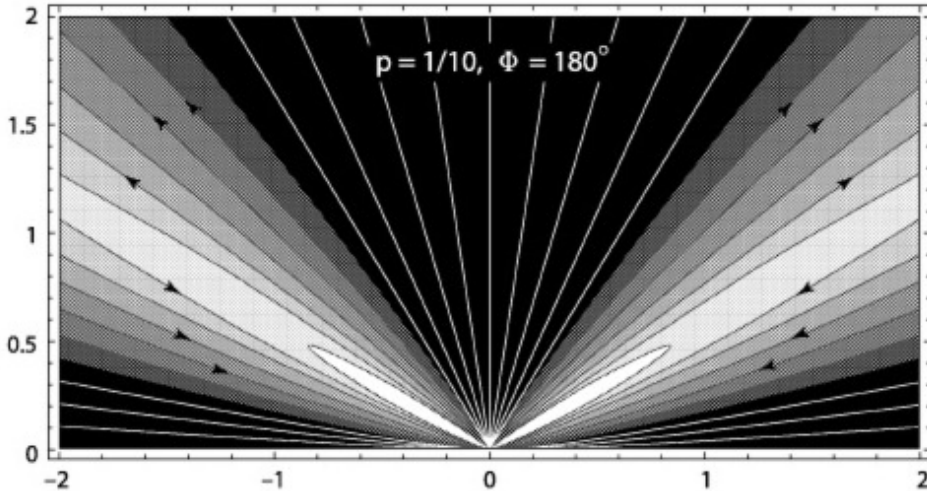


Figure 1. Meridional ingredient of the force-free field of Lynden-Bell & Boily (1994) near the critical condition when a current sheet develops; there is also a corresponding azimuthal component concentrated near the current sheet. Taken from figure 1 of Lynden-Bell MNRAS 341 p 1361.

dinate normals in spherical, cylindrical and planar symmetry.

The question that we consider in this paper is whether these force-free fields can be maintained by a suitable velocity field when resistivity (finite conductivity) effects are taken into account. General aspects of this type of problem have been treated in the review paper of Böström (1973), which gives extensive references to earlier treatments of force-free fields. The limiting current sheet of L-B&B must in reality be subject to the effects of finite conductivity, as in the recent treatment by Bajer & Moffatt (2013) of plane current-sheet formation and dissipation in a tenuous plasma. We shall find that, in a plasma of finite conductivity, the critical angle of twist is not reached; instead, for each member of the family of force-free fields there is a corresponding velocity field by which it can be maintained steadily against ohmic diffusion. Moreover, the required velocity can respond kinematically to a changing force-free field as the defining parameter changes continuously, approaching, but never actually attaining, the flashpoint at which all field lines extend to infinity. Whether such response is dynamically possible requires consideration of the precise relaxation mechanism that tends to maintain a minimum-energy force-free state; this aspect of the problem is beyond the scope of the present paper.

2 FORCE-FREE MAGNETIC FIELDS

2.1 The Grad-Shafranov equation

We first briefly recapitulate the formulation of L-B&B. With spherical polar coordinates $\{r, \theta, \varphi\}$, an axisymmetric magnetic field satisfying $\nabla \cdot \mathbf{B} = 0$ may be expressed in the form

$$\begin{aligned} \mathbf{B}(\mathbf{x}) &= (B_r(r, \theta), B_\theta(r, \theta), B_\varphi(r, \theta)) \\ &= \frac{1}{r \sin \theta} \left(\frac{1}{r} \frac{\partial P}{\partial \theta}, -\frac{\partial P}{\partial r}, r \sin \theta B_\varphi \right), \end{aligned} \quad (2.1)$$

wherein the flux function $P(r, \theta)$ satisfies $(\mathbf{B} \cdot \nabla)P = 0$, so that $P(r, \theta)$ is constant on \mathbf{B} -lines; $2\pi P$ is the flux of \mathbf{B} through any circle $r = \text{cst.}$, $\theta = \text{cst.}$, round the axis of symmetry. In the (non-relativistic) absence of displacement current, the current is given by $\mathbf{j} = \nabla \times \mathbf{B}$, with components

$$j_r = \frac{1}{r \sin \theta} \frac{\partial}{\partial \theta} (\sin \theta B_\varphi), \quad (2.2)$$

$$j_\theta = -\frac{1}{r \sin \theta} \frac{\partial}{\partial r} (r \sin \theta B_\varphi), \quad (2.3)$$

$$j_\varphi = -\frac{1}{r \sin \theta} \left(\frac{\partial^2 P}{\partial r^2} + \frac{\sin \theta}{r^2} \frac{\partial}{\partial \theta} \frac{1}{\sin \theta} \frac{\partial P}{\partial \theta} \right). \quad (2.4)$$

If the Lorentz force $\mathbf{j} \times \mathbf{B}$ dominates over all other forces, then the field must relax instantaneously to a force-free minimum-energy state in which $\mathbf{j} \times \mathbf{B} = 0$; hence

$$\mathbf{j} = \alpha \mathbf{B}, \text{ with } \mathbf{B} \cdot \nabla \alpha = 0, \text{ so that } \alpha = \alpha(P). \quad (2.5)$$

The r - and θ -components of the equation $\mathbf{j} = \alpha\mathbf{B}$ are satisfied provided

$$r \sin \theta B_\varphi = \beta(P), \quad \text{where } \beta'(P) = \alpha(P), \quad (2.6)$$

and, with $\mu = \cos \theta$, the φ -component then gives

$$\frac{\partial^2 P}{\partial r^2} + \frac{1 - \mu^2}{r^2} \frac{\partial^2 P}{\partial \mu^2} = -\beta' \beta; \quad (2.7)$$

this is the pressureless form of the Grad-Shafranov equation (Grad 1958; Shafranov 1966).

The magnetic field in any force-free region is determined in principle by eqns. (2.6) and (2.7) coupled with appropriate boundary conditions. Since these equations don't explicitly involve time or time derivatives, any time dependence is dictated by change in the boundary conditions, through moving of the magnetic field footpoints at the boundary of the force-free region, and the system evolves kinematically in response to such change. Since at each moment the system is in equilibrium, these states can be found by minimising the energy. That method allows calculation of astrophysical jets whose boundaries change (see e.g. Lynden-Bell 2006, 2015).

Here we suppose that the magnetic field is generated by dynamo action within the sphere $r = a$, providing a magnetic flux $2\pi|P|_{\max}$ in each hemisphere, emerging at high latitudes and returning at low latitudes as for a quadrupole field symmetric about the plane $\theta = \pi/2$ and satisfying $B_\theta(r, \pi/2) = 0$; in these circumstances, we may restrict attention to the half-space $0 \leq \theta \leq \pi/2$ (i.e. $1 \geq \mu \geq 0$). For $r > a$, we suppose that the field is axisymmetric and force-free, as described above.

2.2 Similarity solution

Following L-B&B, we seek similarity solutions of (2.7) of the form

$$P(r, \mu) = F(a/r)^p f(\mu), \quad (2.8)$$

where $F = |P|_{\max}^1$. Then $f(\mu)$ satisfies the conditions

$$f(0) = f(1) = 0, \quad f_{\max} = 1. \quad (2.9)$$

This is compatible with (2.7) if $\beta \propto P^m$ where, as easily verified, m must equal $1 + 1/p$. Setting $\beta(P) = \tilde{k}P^{1+1/p}$, we find from (2.6)

$$\alpha = \tilde{k}(1 + 1/p)P^{1/p},$$

¹ If non-dimensional variables $\hat{r} = r/a$ and $\hat{P} = P/F$ are used, then this is equivalent (after dropping 'hats') to setting $a = 1$ and $F = 1$ throughout. Here however, we retain dimensional variables.

i.e.

$$\alpha = \tilde{k}F^{1/p}(1 + 1/p)(a/r)(f(\mu))^{1/p}, \quad (2.10)$$

and eqn. (2.7) reduces to

$$(1 - \mu^2)f''(\mu) = -p(p + 1)f(\mu) - k^2(1 + 1/p)(f(\mu))^{1+2/p}, \quad (2.11)$$

where $k^2 = \tilde{k}^2 F^{2/p} a^2$ is dimensionless.

When $k = 0$ (so that $B_\varphi = 0$) and $p = 2$, the required solution is $f = 3\sqrt{3}\mu(1 - \mu^2)/2$, corresponding to a quadrupole (potential) field for which $|\mathbf{B}|$ decreases like r^{-4} with increasing r ; the flux is outwards for $\mu > 1/\sqrt{3}$ (i.e. $\theta < \pi/3$), inwards for $\pi/3 < \theta < \pi/2$. Increasing k from zero corresponds to increasing B_φ , by means of twist imposed at the boundary $r = a$. The curvature $f''(\mu)$ as given by (2.11) is evidently negative, and, for $p < 2$, k must be just such that $f(\mu)$, starting from zero at $\mu = 0$, returns to zero at $\mu = 1$. When k is so chosen, the maximum of $f(\mu)$ in $0 < \mu < 1$ will in general be some $f_m \neq 1$. However, noting that f/f_m obeys (2.11) with k replaced by $k f_m^{1/p}$, a solution is thus found satisfying the required subsidiary condition $f_{\max} = 1$, albeit with that new k . As p decreases from 2, $\mathbf{B}(\propto r^{-(2+p)})$ extends to increasingly large r , ultimately approaching 'split monopole' r^{-2} behaviour as $p \rightarrow 0$, although still having quadrupole symmetry with respect to the equatorial plane. Numerical solutions for four values of p are shown in Fig. 2. As p decreases, the position of the maximum moves from $\mu = 1/\sqrt{3}$ towards $1/2$, and the curvature $f''(\mu)$ becomes increasingly concentrated near the maximum.

2.3 Asymptotic behaviour

The following asymptotic solution of (2.11) as $p \rightarrow 0$ was obtained by L-B&B (for detailed derivation, see Appendix):

$$f(\mu) = 1 - \frac{p}{p + 1} \ln \cosh [(K/p)(2\mu - 1)], \quad (2.12)$$

where

$$K = k(p + 1)/\sqrt{3} = 1 + (1 + \ln 2)p. \quad (2.13)$$

The corresponding field is $\mathbf{B} = -F a^p r^{-(p+2)} \mathbf{b}(\mu)$, where

$$\begin{aligned} b_r(\mu) &= f'(\mu) = -(2k/\sqrt{3}) \tanh[(K/p)(2\mu - 1)], \\ b_\theta(\mu) &= -p f(\mu)(1 - \mu^2)^{-1/2}, \\ b_\varphi(\mu) &= -\left(\frac{\sqrt{3}K}{p + 1}\right) \frac{(f(\mu))^{(p+1)/p}}{(1 - \mu^2)^{1/2}}. \end{aligned} \quad (2.14)$$

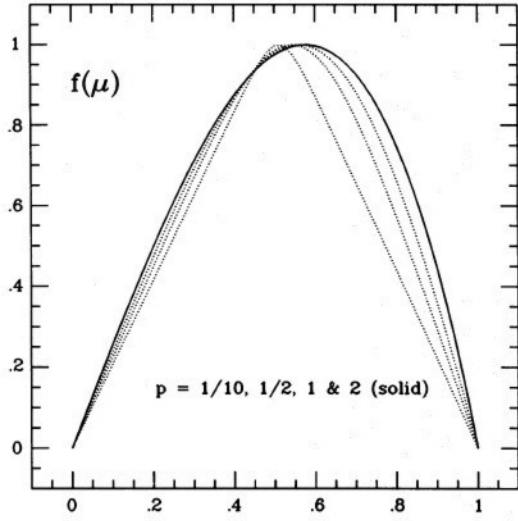


Figure 2. Numerical solutions of eqn. (2.11) for $p = 2, 1, 1/2, 1/10$; as p decreases, the maximum moves from $\mu = 1/\sqrt{3}$ towards $1/2$, and the curvature becomes increasingly concentrated near the maximum. As $p \rightarrow 0$, we get a Λ -shape in the limit. Taken from L-B&B MNRAS 267 p 150.

Here, writing $(p+1)/p = L \gg 1$ and $K/p = \kappa$, we note that

$$\begin{aligned} (f(\mu))^L &= (1 - L^{-1} \ln \cosh[\kappa(2\mu-1)])^L \\ &\sim \exp(-\ln \cosh[\kappa(2\mu-1)]) \\ &= \operatorname{sech}[\kappa(2\mu-1)], \end{aligned} \quad (2.15)$$

so $b_\varphi(\mu)$ (like $b_r'(\mu)$) is clearly concentrated within an $O(\kappa^{-1})$, i.e. $O(p)$, neighbourhood of $\mu = 1/2$.

In what follows we use the asymptotic form (2.12) and give results mainly for the choice $p = 0.1$, representative of the small p situation. For this case, the lower branch of the inverse function, given by

$$\mu(f) = \frac{1}{2} \left[1 - \frac{p}{K} \cosh^{-1} \exp\left(\frac{p+1}{p}(1-f)\right) \right], \quad (2.16)$$

is shown in figure 3 for the relevant range $0 < f < 1$; this inverse function is needed below.

The three field components given by (2.14) are shown in Fig. 4(a); and Fig. 4(b) shows corresponding contributions to $b_r^2 + b_\theta^2 + b_\varphi^2 = M(\mu)$, say. For small p as assumed here, b_θ^2 is negligible, and the variation of b_r^2 is almost compensated by that of b_φ^2 ; in fact, for $p = 0.1$, the variation of $M(\mu)$ from its mean value is not more than ± 3 per cent. This just reflects the near constancy of magnetic pressure across the conical current sheet – not *exactly* constant because of the additional hoop stress associated with curvature of the field lines. Incidentally,

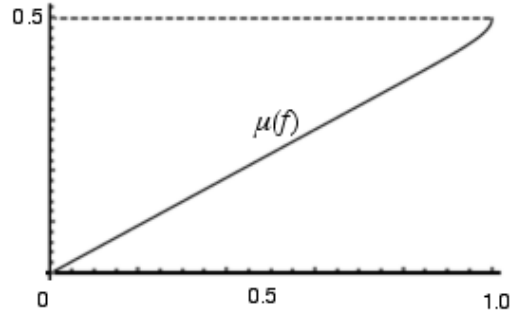


Figure 3. The inverse function $\mu(f)$ (for $p = 0.1$), defined by (2.16).

the constant value of M outside the sheet, M_c say, is given by

$$\begin{aligned} M_c(p) &= 4[1 + (1 + \ln 2)p]^2 / (1+p)^2, \\ &\sim 4 + (8 \ln 2)p + O(p^2) \text{ as } p \rightarrow 0. \end{aligned} \quad (2.17)$$

For $p = 0.1$, this gives $M_c = 4.52$.

The field lines $P(r, \theta) = \text{cst.}$ of the meridional field $\mathbf{B}_m = (B_r, B_\theta, 0)$ are as previously shown in Fig. 1; this is for the choice $p = 0.1$. The field lines here are radially outwards for $0 < \theta < \pi/3$, inwards for $\pi/3 < \theta < \pi/2$, their ‘turnover’ being confined to an $O(p)$ neighbourhood of $\theta = \pi/3$ ($\mu = 1/2$).

3 FIELD MAINTENANCE AGAINST EROSION BY OHMIC DIFFUSION

3.1 Electrostatic potential

We now investigate whether, in a very tenuous conducting medium, the above force-free field can be maintained in a steady state against ohmic diffusion by a suitable velocity field $c \mathbf{u}(\mathbf{x})$, with \mathbf{u} dimensionless². On the surface $r = a$, this velocity field can be prescribed for $0 < \theta < \pi/3$, but at larger θ , it must be compatible with the motions of the conjugate feet of the external field. Ohm’s law in the external medium is

$$\eta \mathbf{j} = \mathbf{E} + \mathbf{u} \times \mathbf{B}, \quad (3.18)$$

where η is the magnetic resistivity, here assumed uniform. Under steady conditions, the electric field \mathbf{E} is derivable from a potential ϕ : $\mathbf{E} = -\nabla\phi$. Hence, with $\mathbf{j} = \nabla \times \mathbf{B} = \alpha \mathbf{B}$, we have

$$\nabla\phi = \mathbf{u} \times \mathbf{B} - \eta\alpha \mathbf{B}, \quad (3.19)$$

² Alternatively, if SI units are used, the velocity field is $\mathbf{u}(\mathbf{x})$, and μ_0 is absorbed in the definition of \mathbf{j} .

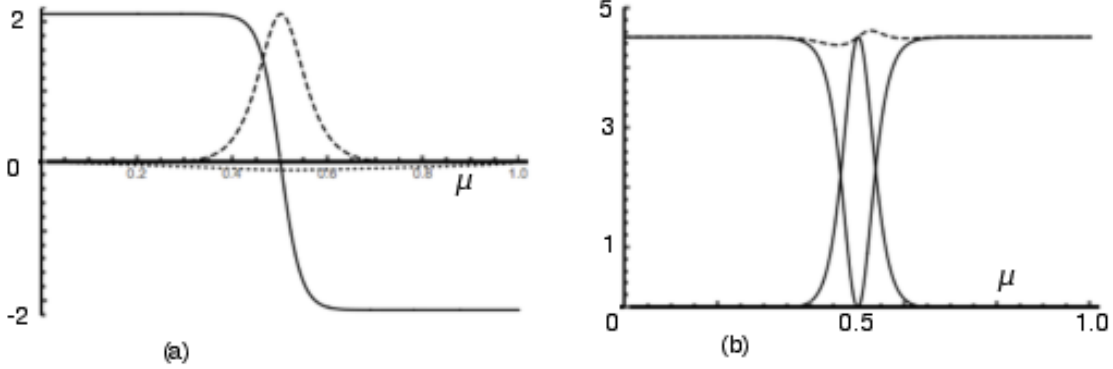


Figure 4. (a) Field components for $p = 0.1$: $b_r(\mu)$ (solid), $b_\theta(\mu)$ (dotted) and $b_\phi(\mu)$ (dashed). (b) Magnetic energy contributions $b_r^2(\mu)$ and $b_\phi^2(\mu)$ (solid) ($b_\theta^2(\mu)$ is negligible), and $M(\mu) = b_r^2 + b_\theta^2 + b_\phi^2$ (dashed). Note the relatively weak variation of $M(\mu)$ across the current sheet.

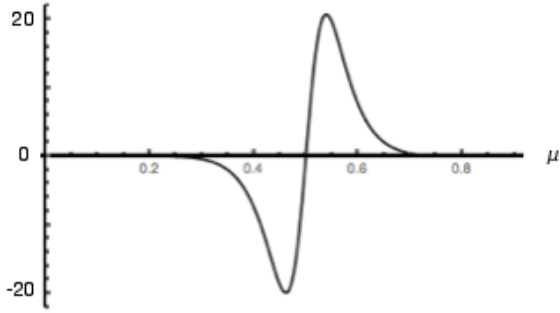


Figure 5. The function $g(\mu)$; $p = 0.1$.

and so

$$(\mathbf{B} \cdot \nabla)\phi = -\eta\alpha\mathbf{B}^2. \quad (3.20)$$

The \mathbf{B} -lines emerge from footpoints on the upper part of the hemisphere $r = a$ where $0 < \theta < \pi/3$, and return to ‘complementary footpoints’ on the lower part where $\pi/3 < \theta < \pi/2$. If $\phi(a, \theta)$ is prescribed for $0 < \theta < \pi/3$, the electrostatic potential $\phi(r, \theta)$ may therefore be found by integrating eqn. (3.20) along \mathbf{B} -lines from one footpoint to the other. However, it is easier to proceed as follows.

3.2 Particular integral

A particular integral of (3.20) may be found in the form

$$\phi_{PI}(r, \theta) = F\eta a^{-2}(a/r)^{p+2}g(\mu), \quad (3.21)$$

© 2015 RAS, MNRAS 000, 1–??

where $g(\mu)$ satisfies

$$\begin{aligned} pf(\mu)g'(\mu) &= (p+2)f'(\mu)g(\mu) \\ &= \sqrt{3}(K/p)(f(\mu))^{1/p}M(\mu). \end{aligned} \quad (3.22)$$

The particular solution of this equation satisfying $g(0.5) = 0$ is antisymmetric about $\mu = 0.5$ and is shown in Fig. 5 for $p = 0.1$; for this solution, $g'(0.5) \approx 918.1$, and $g_{\max} \approx 20.70$ at $\mu \approx 0.539$. Actually, as $p \rightarrow 0$, the asymptotic solution of (3.22) satisfying $g(0.5) = 0$ is given by

$$g(\mu) \sim (2\sqrt{3}/p) \tanh(2\hat{\mu}/p) \operatorname{sech}(2\hat{\mu}/p), \quad (3.23)$$

where $\hat{\mu} = \mu - 0.5$, showing that the lateral scale of $g(\mu)$ around $\mu = 0.5$ decreases in proportion to p while its vertical scale increases like p^{-1} .

To this solution, we may add a complementary function of the form

$$\begin{aligned} g_c(\mu) &= C(f(\mu))^{(p+2)/p} \\ &\approx C\operatorname{sech}^2[\kappa(2\mu - 1)] \quad \text{for } p \ll 1, \end{aligned} \quad (3.24)$$

where C is an arbitrary constant. However, if we prescribe $\phi(a, \mu) = g(\mu)$ for $0 < \mu < 1/2$, then, by the foregoing argument, $\phi(r, \mu)$ is determined everywhere, and is given by

$$\phi(r, \mu) = \phi_{PI}(r, \theta) = F\eta a^{-2}(a/r)^{p+2}g(\mu). \quad (3.25)$$

We shall adopt this pure similarity solution in §4 below.

3.3 Complementary function

However, it may first be useful to indicate how the problem for $\phi(r, \theta)$ may be solved for arbitrary prescription on $\{r = a, 0 < \mu < 1/2\}$.

The ‘complementary function’ ϕ_c of eqn. (3.20)

satisfies $(\mathbf{B} \cdot \nabla)\phi_c = 0$, which simply expresses the fact that ϕ_c is constant on \mathbf{B} -lines. It follows that

$$\phi_c = F\eta a^{-2} \phi_1(\hat{P}), \quad \text{where } \hat{P} = P/F, \quad (3.26)$$

for some function $\phi_1(\hat{P})$. The general solution of eqn. (3.20) is then

$$\phi(r, \mu) = \phi_{PI}(r, \mu) + \phi_c(r, \mu)$$

i.e.

$$\phi(r, \mu) = F\eta a^{-2} \left[(a/r)^{p+2} g(\mu) + \phi_1(\hat{P}) \right]. \quad (3.27)$$

(In the following paragraph, and in figures 6 and 7, the factor $F\eta a^{-2}$ is understood.)

Here, as indicated above, we are free to specify $\phi(r, \mu)$ on the sector $0 < \mu < 1/2$ of the hemisphere $r = a$. By way of example, suppose that $\phi(a, \mu) = 0$ for $0 < \mu < 1/2$, in which case

$$g(\mu) + \phi_1(f(\mu)) = 0 \quad \text{for } 0 < \mu < 1/2. \quad (3.28)$$

In effect, this determines $\phi_1(f)$:

$$\phi_1(f) = -g(\mu(f)), \quad (3.29)$$

where $\mu(f)$ is defined by (2.16). This function and the corresponding function $\phi_c(a, \mu)$ are shown in Fig. 6 (note that $g(\mu(f(\mu))) = g(\mu)$ if $\mu \leq 1/2$, $g(1 - \mu)$ if $\mu \geq 1/2$, symmetric about $\mu = 1/2$); the resulting function $\phi(a, \mu)$, given by (3.27), is shown in Fig. 7(a). The corresponding contours of $\phi(r, \mu)$ in the neighbourhood of the discontinuity at $r/a = 1$, $\mu = 0.5$ are shown in Fig. 7(b).

4 VELOCITY FIELD

4.1 The need for accretion and/or ejection across the surface $r = a$

Returning now to eqn. (3.19), we may solve for \mathbf{u} as a sum of contributions perpendicular and parallel to \mathbf{B} in the form

$$\mathbf{u} = \mathbf{u}_\perp + \mathbf{u}_\parallel = B^{-2} \mathbf{B} \times \nabla \phi + \gamma(r, \theta) \mathbf{B}, \quad (4.30)$$

where $\gamma(r, \theta) = \mathbf{u} \cdot \mathbf{B}/B^2$ is an undetermined scalar field. Here, $\mathbf{u}_\perp = \mathbf{E} \times \mathbf{B}/B^2$ is the ‘plasma drift velocity’ and is explicitly determined in terms of \mathbf{B} and ϕ as given by (2.14) and (3.25); it is finite everywhere and $O(r^{-1})$ as $r \rightarrow \infty$.

The radial component of \mathbf{u} is

$$u_r = -\frac{1}{B^2} \frac{B_\varphi}{r} \frac{\partial \phi}{\partial \theta} + \gamma B_r, \quad (4.31)$$

and if we were to require that $u_r = 0$ on $r = a$, then we would have $\gamma(a, \mu) = (B_\varphi/B^2 B_r) \partial \phi / \partial \theta$ which is infinite at $\mu = 1/2$ where $B_r = 0$ (and $\partial \phi / \partial \theta \neq 0$). The θ and ϕ components of \mathbf{u} ,

$$u_\theta = \frac{1}{B^2} B_\varphi \frac{\partial \phi}{\partial r} + \gamma B_\theta,$$

$$u_\phi = \frac{1}{B^2} \left(\frac{B_r}{r} \frac{\partial \phi}{\partial \theta} - B_\theta \frac{\partial \phi}{\partial r} \right) + \gamma B_\phi, \quad (4.32)$$

are then both infinite at $\mu = 1/2$ (where $B_\theta \neq 0$, $B_\varphi \neq 0$). If such infinities are to be avoided, then we simply cannot impose the condition $u_r = 0$ on $r = a$: there must be some flow (accretion and/or ejection) across this surface.

4.2 Purely radial meridional velocity field

The simplest situation is in fact that in which the meridional velocity field is purely radial, i.e. $u_\theta(r, \mu) = 0$. From (4.32), this occurs for the choice

$$\gamma(r, \mu) = -\frac{B_\varphi}{B_\theta B^2} \frac{\partial \phi}{\partial r} = (\eta a/F)(r/a)^{p+1} \hat{\gamma}(\mu), \quad (4.33)$$

with

$$\hat{\gamma}(\mu) = (p+2) \frac{b_\varphi(\mu)g(\mu)}{b_\theta(\mu)M(\mu)}. \quad (4.34)$$

The radial velocity in this special case is however most easily obtained directly from the φ -component of (3.19) which gives

$$u_r(r, \mu) = \eta \alpha B_\varphi / B_\theta = (\eta/r) v_r(\mu), \quad (4.35)$$

where, with $\hat{\mu} = \mu - 1/2$,

$$v_r(\mu) = \frac{3K^2}{p^2(p+1)} (f(\mu))^{2/p} \sim \frac{3}{p^2} \text{sech}^2(2\hat{\mu}/p) \quad (4.36)$$

as $p \rightarrow 0$. This radial velocity has a conical-jet-like structure, symmetric about $\mu = 1/2$, and with $v_r|_{\max} \sim p^{-2}$ as $p \rightarrow 0$. The function $p^2 v_r(\mu)$ is shown in Fig. 8(a) for $p = 0.1$ and $p = 0.025$; note how the jet becomes more concentrated around the cone $\mu = 1/2$ (in proportion to p) as p decreases.

Similarly, under the condition $u_\theta(r, \mu) = 0$, the azimuthal (or ‘twist’) component of velocity is given from the radial component of (3.19), i.e.

$$-u_\varphi B_\theta = \partial \phi / \partial r - \eta \alpha B_r, \quad (4.37)$$

giving $u_\varphi(r, \mu) = (a/r) v_\varphi(\mu)$ where

$$v_\varphi(\mu) = \frac{(p+2)g(\mu) - (\sqrt{3}k/p)(f(\mu))^{1/p} f'(\mu)}{b_\theta(\mu)} \quad (4.38)$$

with asymptotic form

$$v_\varphi(\mu) \sim -(3\sqrt{3}/p^2) \tanh(2\hat{\mu}/p) \text{sech}(2\hat{\mu}/p), \quad (4.39)$$

as $p \rightarrow 0$. Hence v_φ , like v_r , scales like p^{-2} as $p \rightarrow 0$. The function $v_\varphi(\mu)$ is shown in Fig. 8(b) again for $p = 0.1$ and $p = 0.025$; note again the increase of amplitude and decrease of scale as p decreases. We note further that, in this situation, the equation of mass conservation is simply $(\partial/\partial r)(r\rho(r, \mu)v_r(\mu)) = 0$, so that any density field of the form $\rho(r, \mu) = r^{-1} \hat{\rho}(\mu)$ remains steady under the action of this velocity field. Interestingly, with this density distribution, we may,

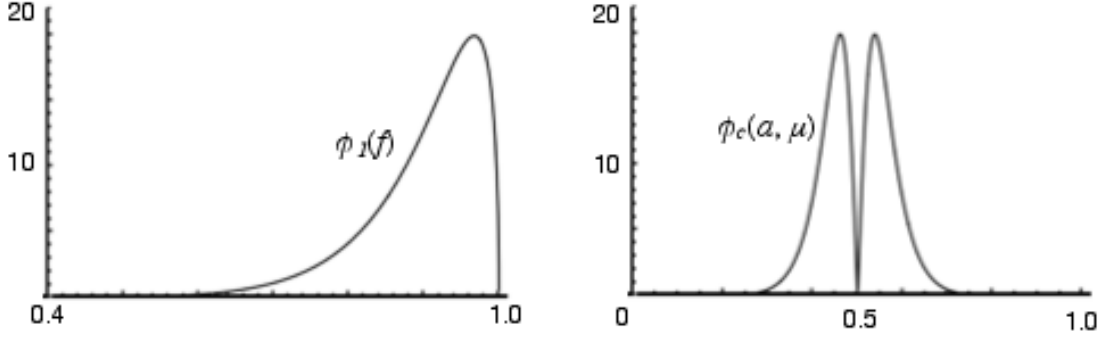


Figure 6. The functions $\phi_1(f)$ and $\phi_c(a, \mu) = \phi_1(f(\mu))$.

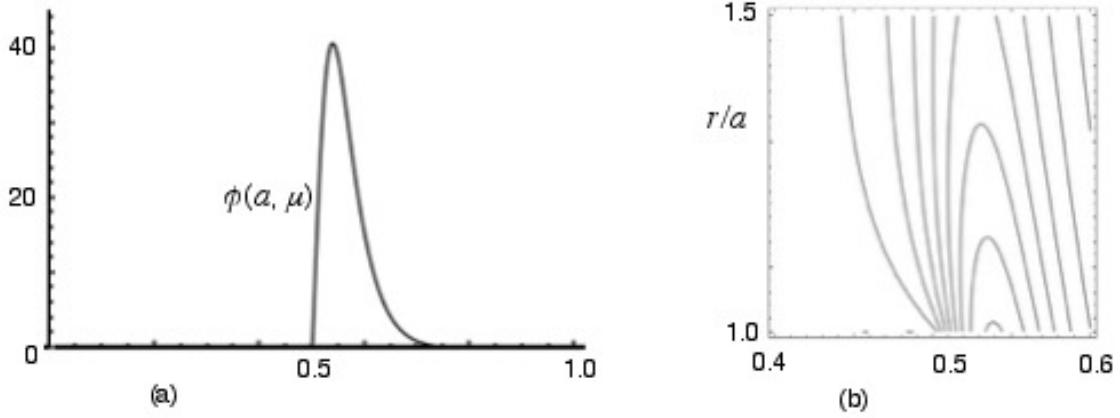


Figure 7. (a) The function $\phi(a, \mu)$, given by (3.27); imposition of the condition $\phi(a, \mu) = 0$ for $0 < \mu < 0.5$ determines $\phi(a, \mu)$ over the rest of the range $0.5 < \mu < 1$. (b) Corresponding contours of $\phi(r, \mu)$ for $1 < r/a < 1.5$ (vertical), $0.4 < \mu < 0.6$ (horizontal).

without affecting the density field, add a velocity parallel to \mathbf{B} of the form

$$\Delta \mathbf{u} = U(P)\mathbf{B}/\rho(r, \mu), \quad (4.40)$$

which, for arbitrary $U(P)$, satisfies

$$\nabla \cdot (\rho \Delta \mathbf{u}) = \nabla \cdot (U(P)\mathbf{B}) = U'(P)(\mathbf{B} \cdot \nabla)P = 0. \quad (4.41)$$

4.3 General structure of the transverse velocity field $\mathbf{u}_\perp = \mathbf{E} \times \mathbf{B}/B^2$

From (4.31) and (4.32), the components of \mathbf{u}_\perp are

$$u_{\perp r} = -\frac{1}{B^2} \frac{B_\varphi}{r} \frac{\partial \phi}{\partial \theta},$$

$$\begin{aligned} u_{\perp \theta} &= \frac{1}{B^2} B_\varphi \frac{\partial \phi}{\partial r}, \\ u_{\perp \phi} &= \frac{1}{B^2} \left(\frac{B_r}{r} \frac{\partial \phi}{\partial \theta} - B_\theta \frac{\partial \phi}{\partial r} \right). \end{aligned} \quad (4.42)$$

Hence, $\mathbf{u}_\perp = (\eta a/r)\mathbf{v}_\perp(\mu)$, where, adopting (3.25),

$$v_{\perp r}(\mu) = b_\varphi(\mu)(1 - \mu^2)^{1/2} g'(\mu)/M(\mu),$$

$$v_{\perp \theta}(\mu) = -(p+2)b_\varphi(\mu)g(\mu)/M(\mu),$$

$$v_{\perp \phi}(\mu) = [-b_r(\mu)(1 - \mu^2)^{1/2} g'(\mu)$$

$$+(p+2)b_\theta(\mu)g(\mu)]/M(\mu).$$

For small p , and still with $\hat{\mu} = \mu - 1/2$, the leading terms in the asymptotic expansions of these

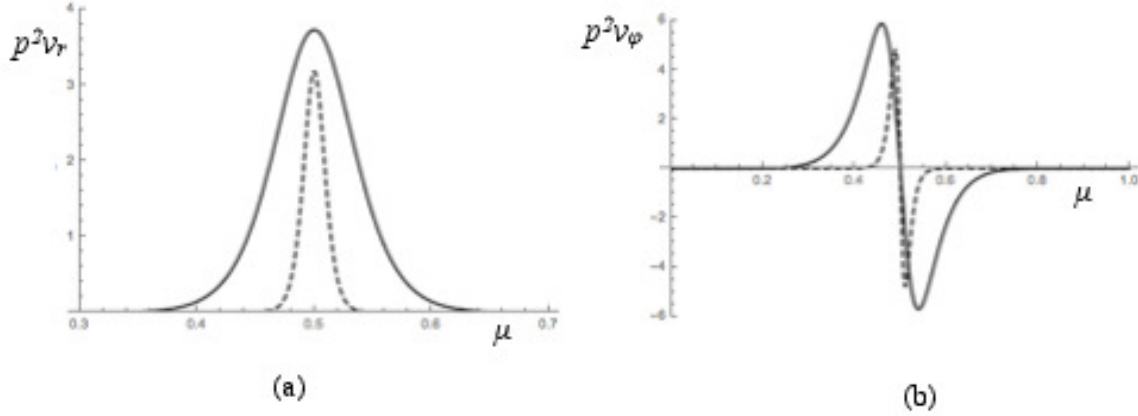


Figure 8. (a) The function $p^2 v_r(\mu)$ for $p = 0.1$ (solid) and $p = 0.0125$ (dashed), showing a jet-like structure; as p decreases, the maximum velocity scales asymptotically like p^{-2} , and the lateral scale decreases in proportion to p . (b) The same for the associated scaled twist component of velocity $p^2 v_\phi(\mu)$.

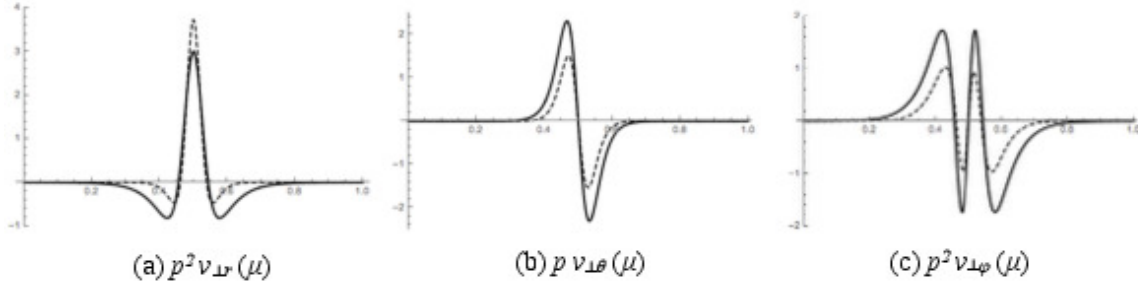


Figure 9. The components $v_{\perp r}(\mu)$, $v_{\perp \theta}(\mu)$, $v_{\perp \phi}(\mu)$, scaled by the factors p^2 , p , p^2 respectively. The dashed curves in each case correspond to the exact results for $p = 0.1$, and the solid curves are the asymptotic results (4.43).

expressions are:

$$\begin{aligned} v_{\perp r} &\sim (3/p^2)(1 - \sinh^2(2\hat{\mu}/p))\text{sech}^4(2\hat{\mu}/p), \\ v_{\perp \theta} &\sim -(6/p)\sinh(2\hat{\mu}/p)\text{sech}^3(2\hat{\mu}/p), \\ v_{\perp \phi} &\sim \frac{4\sqrt{3}\sinh(2\hat{\mu}/p)(1 - \sinh^2(2\hat{\mu}/p))}{p^2 \cosh^3(2\hat{\mu}/p)}. \end{aligned} \quad (4.43)$$

Note particularly that $u_{\perp r}(\mu)$ and $u_{\perp \phi}(\mu)$ are both $O(\eta/p^2)$ as $p \rightarrow 0$, whereas $u_{\perp \theta}(\mu)$ is $O(\eta/p)$; however, the contributions $u_{\perp r}(\mu)B_\theta$ and $-u_{\perp \theta}(\mu)B_r$ to the electromotive force component $(\mathbf{u}_{\perp} \times \mathbf{B})_\phi$ are both $O(\eta/p^2)$. These velocity components are shown in Fig. 9; the dashed curves are the exact results for $p = 0.1$, and the solid curves are the leading terms (4.43) also evaluated at $p = 0.1$. Note the scaling factors p^2 and p . The difference between the dashed and solid curves is an indication of slow approach to the asymptotic behaviour as $p \rightarrow 0$.

The θ -component of velocity is, from both sides, towards the current sheet centred on $\mu = 1/2$, and there is a much stronger r -component, also centred on this sheet, with net flux outwards. The ϕ -component is also strong, and has a more complex structure here than that shown in figure 8, where the meridional flow was purely radial. Again however, the flow may be described as having a ‘swirling conical jet’ character.

5 DISCUSSION

We have shown that each of the one-parameter family of force-free self-similar magnetic fields found by L-B&B can be steadily maintained in a medium of finite conductivity against the effects of ohmic diffusion by fluid flow, having both meridional and twist

(i.e. toroidal) components. When the parameter p is small, the velocity is concentrated in a region of small angular extent $O(p)$ centred on the cone $\mu = \cos \theta = 1/2$, and its magnitude scales like p^{-2} . The simplest possibility, as described in §4.2, is that the meridional flow is purely radial; much of this flow is the driven $\mathbf{E} \times \mathbf{B}/B^2$ drift; it has a conical jet-like structure, as shown in Fig. 8(a), and the associated twist component of velocity is antisymmetric about $\mu = \cos \theta = 1/2$ (Fig. 8(b)).

There remains the question of how the component along the field can be driven dynamically. One possible mechanism is that magnetic diffusion in fact causes a small spread of b_φ^2 from the form shown in figure 4(b) and so a small dip in magnetic pressure near the cone $\mu = 0.5$; this could then be compensated by an increase of plasma density and pressure in this region, the resulting radial pressure gradient being just sufficient to maintain the conical jet flow. To treat this effect properly would require a dynamical analysis of a tenuous finite-conductivity plasma (cf Bajer & Moffatt 2013), taking due account of the relaxation mechanism by which the nearly force-free state is maintained.

The radial flow emerges from the sphere $r = a$ and must carry toroidal flux across its surface. Both $u_r B_\varphi$ and ρu_r must be continuous across the surface, so B_φ/ρ must be continuous, implying a large internal B_φ , if the density drops significantly across $r = a$.

A further consideration is that a current sheet is in general susceptible to resistive instabilities (Furth, Killeen & Rosenbluth, 1963). Here, such instabilities will be influenced by the associated flow field \mathbf{u} , but are still to be expected when the sheet is sufficiently thin, i.e. when p is sufficiently small. The effect of these instabilities must be to cause reconnection of the magnetic field across the sheet, with consequent detachment and ejection of the outer part of the field, a process that will presumably be accelerated by the pre-existing outward conical jet flow. With persistent twisting of the inner region, the sheet will then reform and it may be conjectured that the reconnection and ejection process will occur repetitively. This type of scenario, first conceived by Aly (1986, section 3C), deserves further investigation; if confirmed, it will have important astrophysical implications.

The model treated in this paper may have application to accretion discs, and the mechanism by which jets from accretion discs are formed. Such jets are generally observed to be axial rather than conical, but the mechanism by which they are formed is by no means fully understood. The present paper may provide a small step towards a better understanding of this process.

REFERENCES

- Aly, J.J., 1984, On some properties of force-free magnetic fields in infinite regions of space. *ApJ*, 283, 349-362
- Aly, J.J., 1986, Some topics in the magnetohydrodynamics of accreting magnetic compact objects. *AIP Conference Proceedings* 144, 45.
- Aly, J.J., 1994, Asymptotic formation of a current sheet in an indefinitely sheared force-free field; an analytic example. *A&A*, 288, 1012-1020
- Aly, J.J., 1995, Non-equilibrium in sheared axisymmetric force-free magnetic fields. *ApJ*, 439, L63-L66
- Bajer, K., Moffatt, H.K., 2013, Magnetic relaxation, current sheets, and structure formation in an extremely tenuous fluid medium. *ApJ*, 779, 169-183
- Böstrom, R., 1973, Models of force-free magnetic fields in resistive media. *Astrophysics and Space Science* 22.2, 353-380
- Furth, H.P., Killeen, J., Rosenbluth, M.N., 1963, Finite-resistivity instabilities of a sheet pinch. *Phys. Fluids* 6, 459
- Gourgouliatos, K.N., 2008, Self-similar magnetic arcades. *MNRAS*, 385, 875-882
- Grad, H., Rubin, H., 1958, Hydromagnetic equilibria and force-free fields. *Proc. 2nd UN Conf. on the Peaceful Uses of Atomic Energy*, f 31, Geneva: IAEA p. 190
- Lynden-Bell, D., 2006, Magnetic jets from swirling discs. *MNRAS*, 369, 1167-1188
- Lynden-Bell, D., 2015, Jets at birth and death. In *The Formation and Disruption of Black Hole Jets*, Springer, 1-24 Eds. Contopoulos, I. Gabuzda, D., Kylafis, N., *Astrophysics and Space Science Library*, 414, Springer, pp 1-24
- Lynden-Bell, D., Boily, C., 1994, Self-similar solutions up to flashpoint in highly wound magnetostatics. *MNRAS*, 341, 146-152
- Shafranov, V.D., 1966, Plasma equilibrium in a magnetic field, *Rev. Plasma Phys.* 2, New York: Consultants Bureau, p. 103

APPENDIX A: ASYMPTOTIC SOLUTION OF EQN. (2.11)

With $p \ll 1$, we may at leading order neglect the term $-p(p+1)f(\mu)$ in (2.11). Let μ_m be the point at which $f(\mu)$ is maximal, with $f'(\mu_m) = 0$. Then, with p small, $f^{1+2/p}$, and so $f''(\mu)$, are both small everywhere except close to μ_m . To exploit this, we write $1 - \mu^2 = 1 - \mu_m^2 - (\mu^2 - \mu_m^2)$ in eqn. (2.11), multiply by $2f'(\mu)$, and integrate from μ_m to μ , obtaining

$$(1 - \mu_m^2)f'^2 = k^2(1 - f^{2L}) + I(\mu), \quad (\text{A1})$$

where $L = 1 + 1/p \gg 1$, and

$$I(\mu) = 2 \int_{\mu_m}^{\mu} (\mu^2 - \mu_m^2) f'(\mu) f''(\mu) d\mu. \quad (\text{A2})$$

Now near μ_m , $I(\mu)$ is of order $(\mu - \mu_m)^3$ which is smaller than the other terms, while away from this it contains $f''(\mu)$ which we have shown to be small. Thus I is small everywhere and may be neglected at leading order; (it may be verified retrospectively that $I(\mu) = O(p)$ in the limit $p \rightarrow 0$). We then have

$$(1 - f^{2L})^{-1/2} df = k(1 - \mu_m^2)^{-1/2} d\mu. \quad (\text{A3})$$

With the substitution $f(\mu) = 1 - L^{-1} \ln y(\mu)$, $df = -dy/Ly$, and noting that for L large

$$f^L = [1 - L^{-1} \ln y]^L \sim \exp(-\ln y) = 1/y, \quad (\text{A4})$$

we find

$$dy/\sqrt{y^2 - 1} = -\kappa d\mu \text{ where } \kappa = Lk/\sqrt{1 - \mu_m^2}. \quad (\text{A5})$$

This integrates to give $y = \cosh[\kappa(\mu - \mu_m)]$ and hence, asymptotically,

$$f = 1 - L^{-1} \ln \cosh[\kappa(\mu - \mu_m)]. \quad (\text{A6})$$

Applying the boundary conditions $f(0) = f(1) = 0$, we find that $\mu_m = 1/2$ and $\ln \cosh(\kappa/2) = L$. Hence, for small p (large L), $\kappa \sim 2(L + \ln 2)$ and so $k \sim \sqrt{3}[1 + \ln 2/L]$. These results are equivalent to (2.12) and (2.13), as used in the main text.

This paper has been typeset from a $\text{\TeX}/\text{\LaTeX}$ file prepared by the author.